Plate 3. CZCS-derived chl Climatological Monthly Means

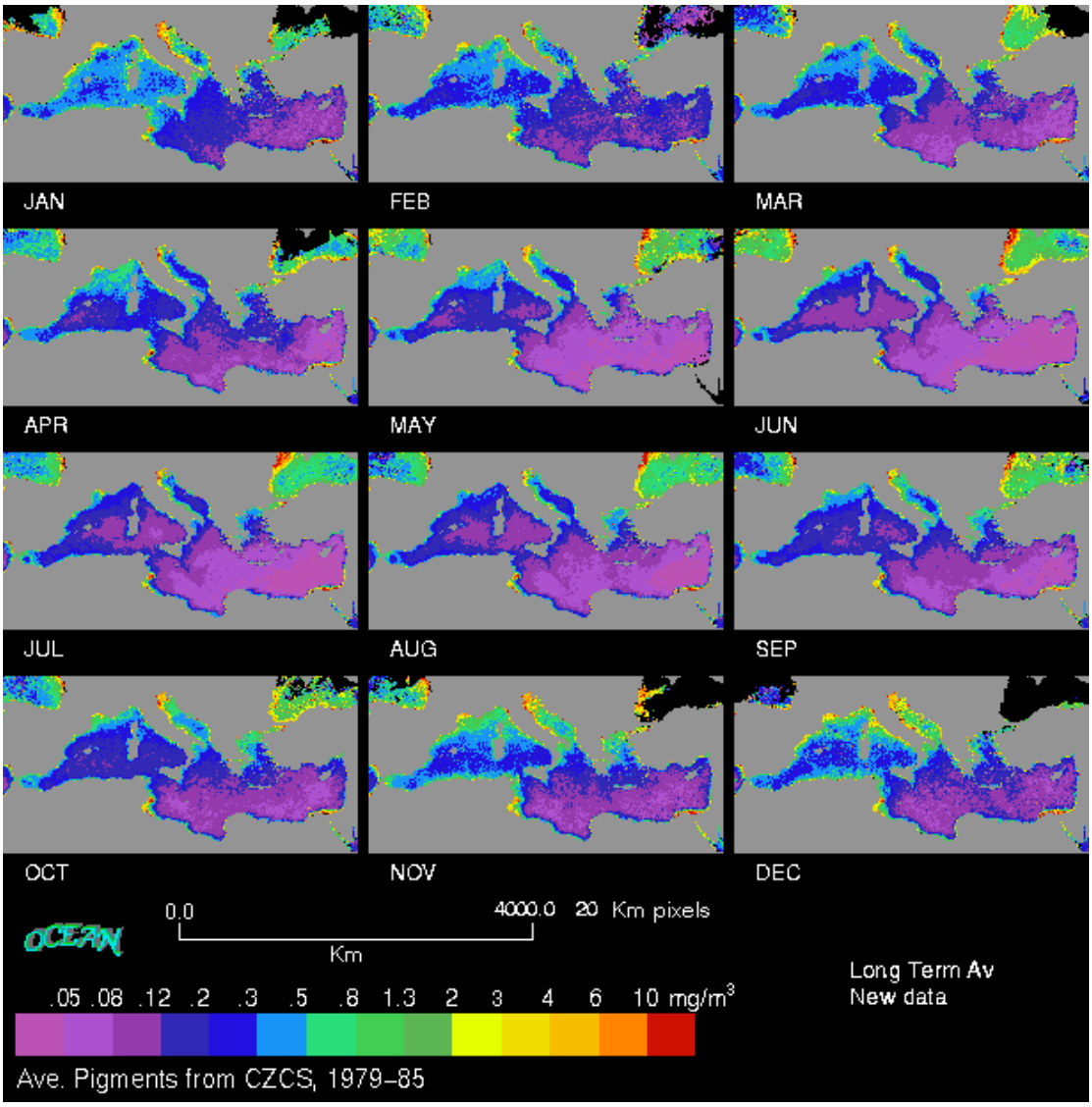

2. Interannual variability

The assessment of interannual variability in the 1998-2003 SeaWiFS-derived data set was carried out by generating annual means of *chl* and then comparing each year with the climatological data derived for the same period. The climatological annual mean (Plate 4) was computed as the average of the annual means derived for each of the 6 years available (Plate 5). Each of these, in turn, was computed both as the average of the 12 monthly means considered with equal weight, as well as the average of the monthly means weighted by the number of observations available on a pixel-by-pixel basis. A comparison by linear regression of the values obtained for each year with the two methods shows a correlation coefficient ranging from 0.9946 to 0.9965 (Plate 6), thus testifying that, in spite of the irregular coverage provided by SeaWiFS in the years considered, given the high number of realizations used to compute the averages, the mean images are only marginally affected by the specific weighting function adopted. The evaluation of interannual variability was done by computing *chl* anomalies at the annual scale, as the difference between each individual year and the climatological year. The results were mapped for each pixel both as percent as well as real values (Plate 8).

2.2 Spatial patterns in the annual means

The oligotrophic character of most sub-basins is the main feature of the Mediterranean Sea appearing in the climatological annual mean of Plate 4. The western and eastern basins are not too dissimilar, in the offshore (pelagic) domain, with an overall basin average of *chl* around 0.2 mg m^{-3}. The inshore (near-coastal) domain, on the other hand, presents higher *chl* values in the northwest and west, and lower *chl* values in the south and southeast. The high-*chl* near-coastal areas include the Ligurian–Provençal–Balearic sub-basins, and the (northern) Adriatic and Aegean Seas. This rim of enhanced pigments around most of the northern Mediterranean is associated with the impact of runoff from continental margins (*i.e.* both a direct impact due to the sediment load and one induced on the plankton flora by the associated nutrient load), but may reflect also the vertical mixing regime due to the prevailing winds, *i.e.* the Mistral over the north-western Mediterranean, the Bora over the Adriatic and the Etesians over the Aegean (Barale and Zin, 2000). Other examples of dynamical features related to mixing processes in the water column are provided by the quasi-permanent gyres due to the incoming Atlantic jet in the Alboran Sea, or by the giant filament of Capo Passero, at the southern tip of Sicily, also linked to the current system originated by the Atlantic jet flowing eastward over a steep continental slope. Where major rivers (*i.e.* the Ebro, Rhone, Po, in the western basin and the Nile, in the eastern basin) flow into the basin, coastal areas appear to be permanently under the direct influence their plumes, a feature that was already evident in the CZCS historical data set (Barale and

Larkin, 1998). Minor river discharges, or non-point sources of runoff, also have a coastal signature in the pigment field, as along the Italian coast in the Tyrrhenian Sea, along both the Italian and Albanian coastlines in the Adriatic Sea, and along the northern shores of the Aegean Sea and the Marmara Sea, where exchanges with the Black Sea also take place. In the coastal area off southern Tunisia, instead, the enhanced pigment signal is due to direct bottom reflection in an area of shallow clear waters, around the Kerkenna Island, and not to runoff patterns (Jaquet *et al.*, 1999).

The features of the climatological annual mean image appear to be recurrent in the single annual means of Plate 5. However, a certain degree of interannual variability is evident in the main spatial patterns. In particular, the size of the blooming area in the northwestern sub-basin (with *chl* ≥ 0.3 mg m^{-3}) appears to increase from 1998 to 1999, but then to decrease systematically from 2000 to 2003. Similarly, the size of the super-oligotrophic area in the southeastern sub-basin (with *chl* << 0.1 mg m^{-3}) appears to increase systematically in the second half of the period covered by SeaWiFS. This is reflected in the variability of the average basin value of *chl* derived from the annual means (*i.e.* a single *chl* value computed as the total average of all pixels composing each annual image) shown in Plate 7. The trend appearing in this variability indicates a general decrease in the *chl* indicator, over the period of SeaWiFS coverage, estimated to be about 10% of the climatological average value for the entire basin.

2.2 Blooming Anomalies in the Annual Means

The SeaWiFS-derived *chl* annual anomalies shown in Plate 8 highlight the geographical spread and intensity of blooming patterns, which differed in each year from the climatological annual mean. The basin shows mostly positive anomalies in the first 3 years and mostly negative anomalies in the second 3 years. The northwestern sub-basin displays a *quasi*-systematic counter-trend, with respect to the remainder of the western basin, both in a negative sense, as in 1998-1999, as well as in a positive sense, as in 2002. The northeastern sub-basin also seems to show a recurring counter-trend, with respect to the eastern basin, again both in a negative sense, as in 1998-1999, as well as in a positive sense, as in 2003. Inshore areas can also present sharp fluctuations (absolute value ≥ 0.1 mg m^{-3}) from negative to positive anomalies, and *vice versa*, as apparent along the Catalan coast or in the northern Adriatic sea (see *e.g.* 1998 *vs* 2003, in both cases). Very high anomalies (absolute value ≥ 10 mg m^{-3}), labeled in Plate 8 as "excess anomalies", are seen to recur only along the shoreline, in shallow waters (near the Island of Jerba) or around river plumes (south of the Po river delta).

Plate 4. SeaWiFS-derived chl Climatological Annual Mean

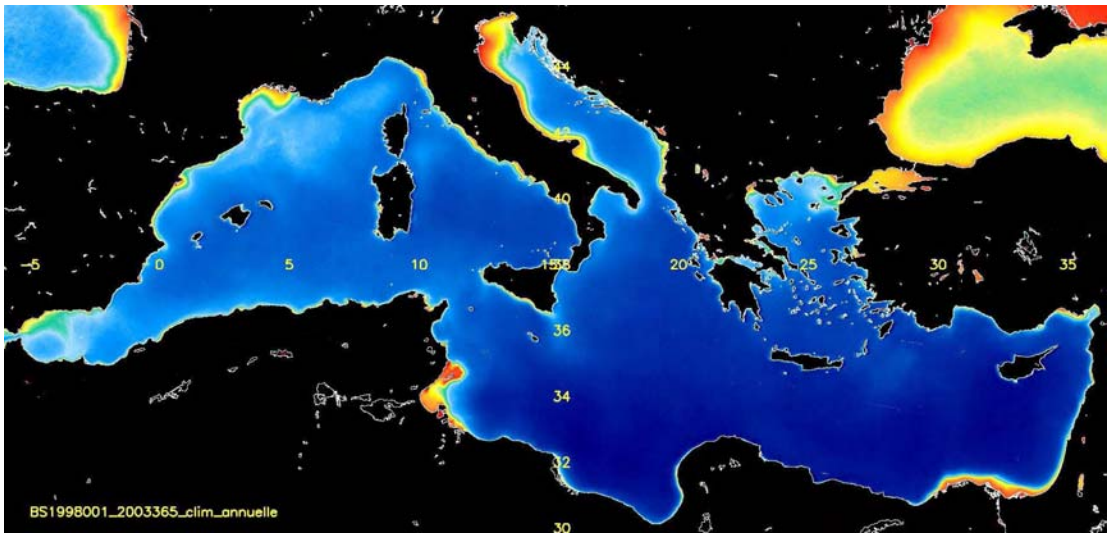

climatological annual mean

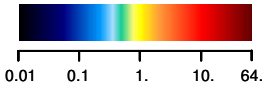

chl [mg m^{-3}]

Plate 5. SeaWiFS-derived chl Annual Means

annual mean 1998

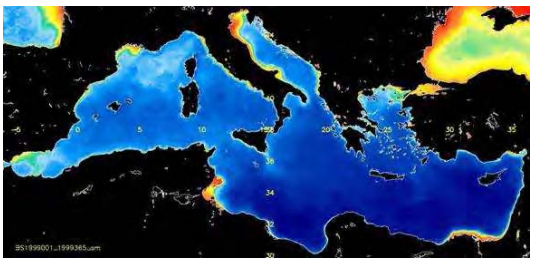

annual mean 1999

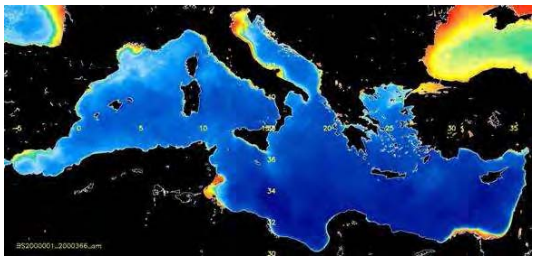

annual mean 2000

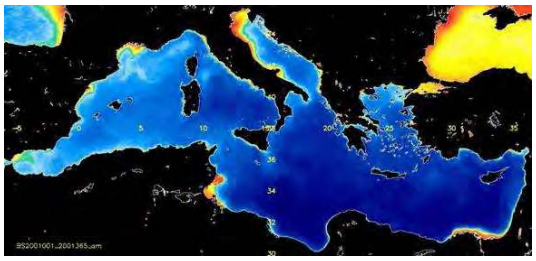

annual mean 2001

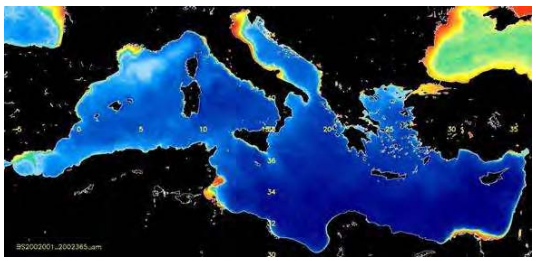

annual mean 2002

annual mean 2003

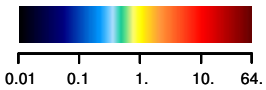

chl [mg m^{-3}]

Plate 6. Annual Mean chl vs Annual Weighted Mean chl

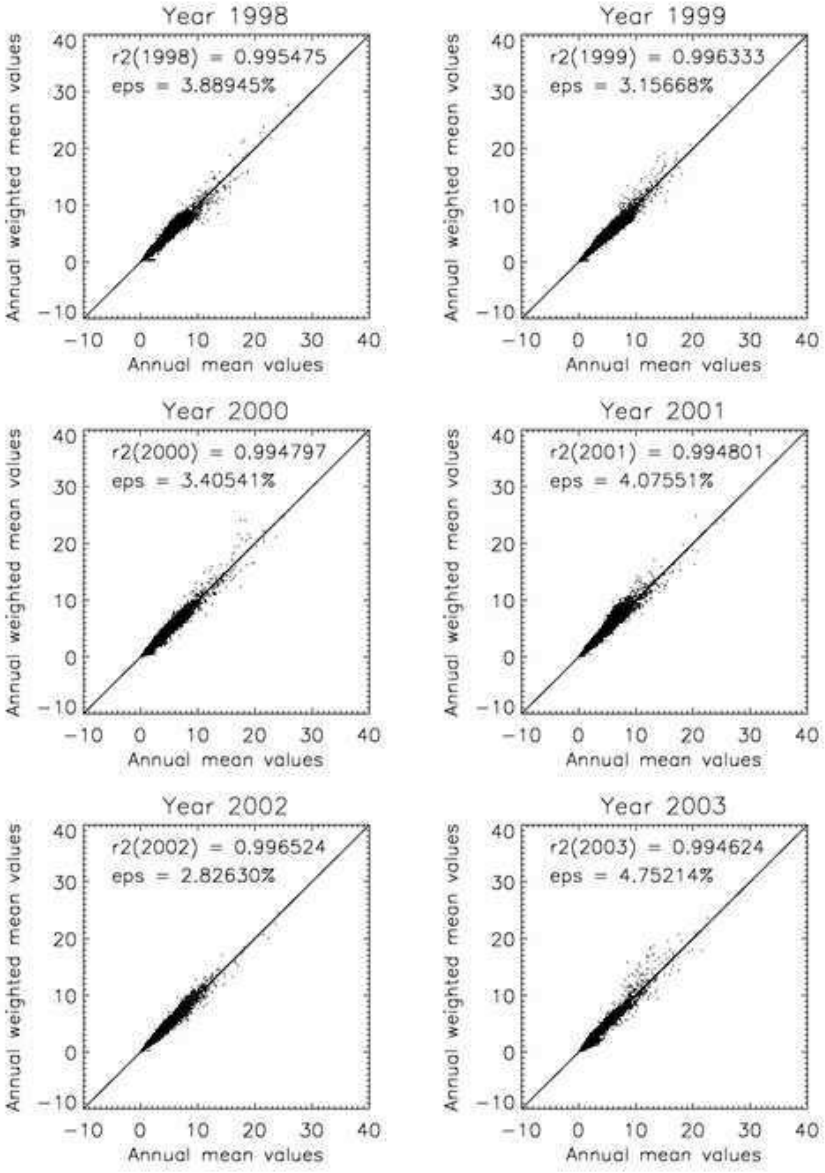

Plate 7. Trend of the chl Annual Means (average basin value)

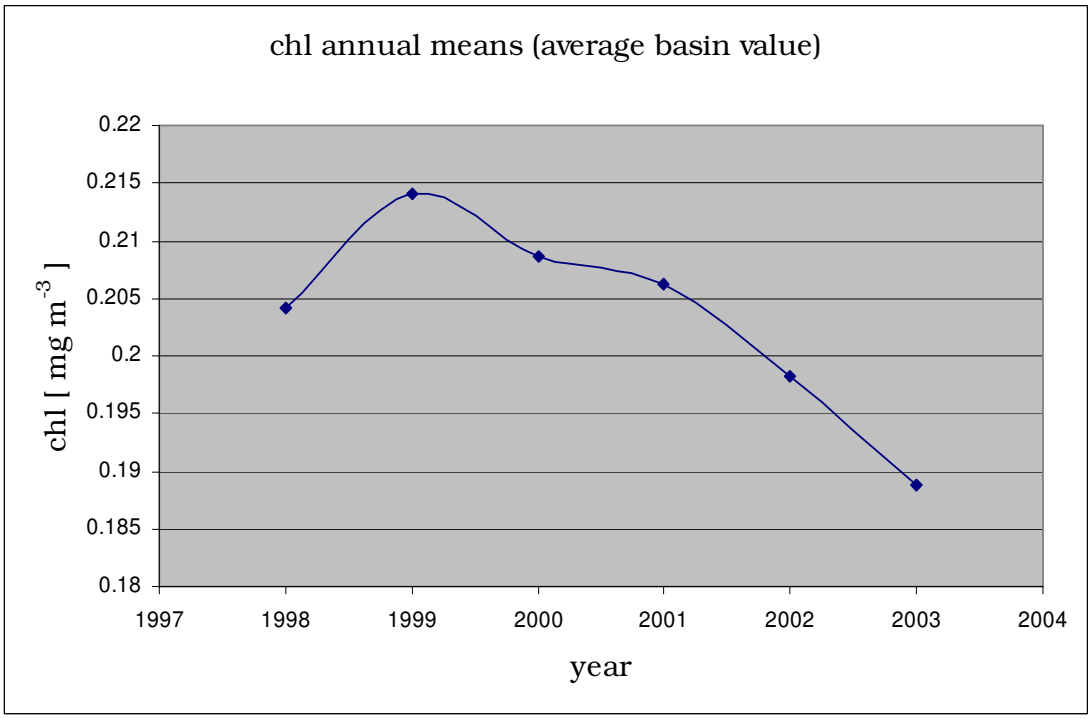

Plate 8. SeaWiFS-derived chl Annual Anomalies

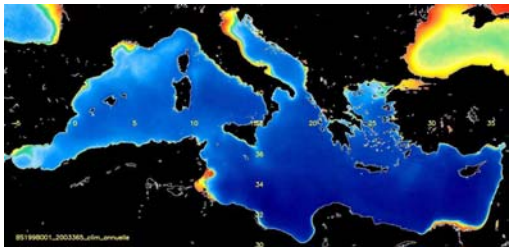

climatological annual mean

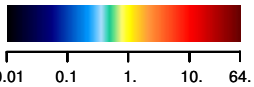

chl [mg m^{-3}]

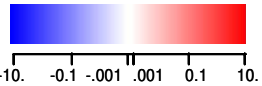

anomalies [mg m^{-3}]

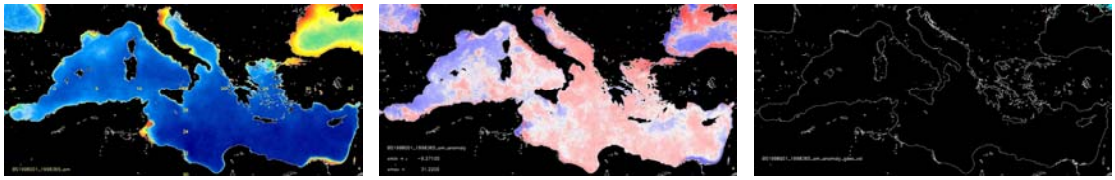

1998

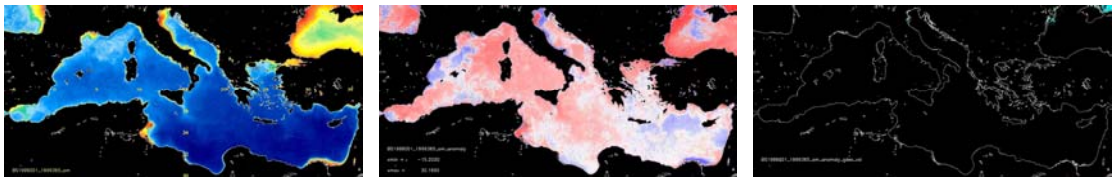

1999

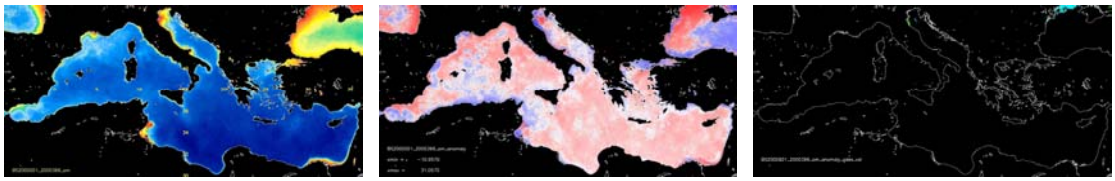

2000

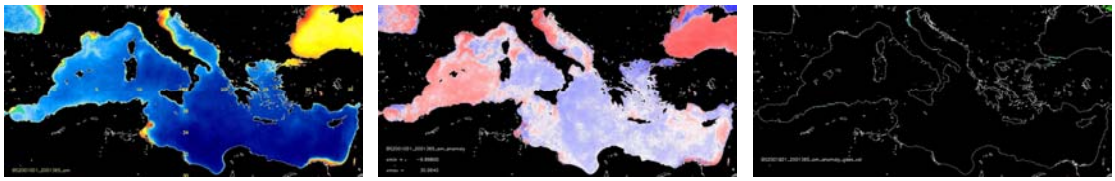

2001

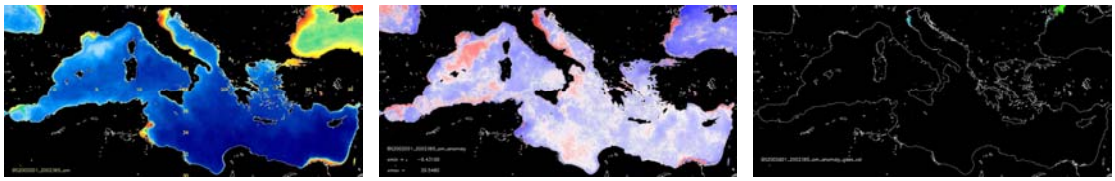

2002

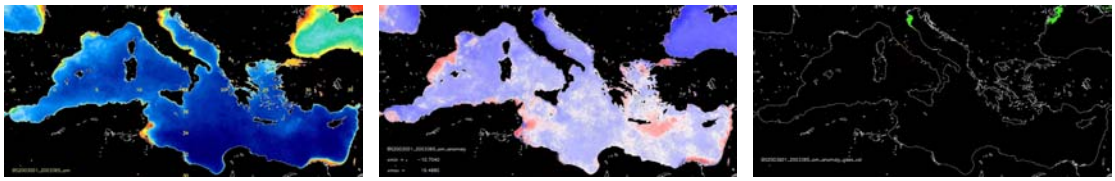

2003

Left panels: annual mean concentration of chl [mg m^{-3}]
Middle panels: chl anomalies [mg m^{-3}] as mean concentration – climatological value
Right panels: excess anomalies (blue < -1 mg m^{-3}, green > +1 mg m^{-3})

3. Seasonal variability

The assessment of seasonal variability in the 1998-2003 SeaWiFS-derived data set was carried out by generating climatological monthly means of *chl* (*i.e.* 12 monthly means generated as the average of the 6 realizations available for each month in the period 1998-2003; see Plate 9), and then comparing single monthly means with the climatological record. Thus, a time component was coupled to the evaluation of space patterns, by computing the sequence of *chl* anomalies at the monthly scale, as the difference between each individual month and the corresponding climatological month. Again, the results were mapped for each pixel, both as percent as well as real values (Plates 13 to 24). As in the annual case, "excess" anomalies (absolute value ≥ 10 mg m^{-3}), generally recurring for pixels in near-coastal areas, were also mapped separately, in order to retain a first order assessment of potential hot spots, both in space and time, for anomalous blooming.

3.1 Spatial Patterns and Trends in the Monthly Means

The spatial patterns appearing in the climatological monthly means of Plate 9 are not dissimilar from those observed at the annual scale, but show enhancements over (variable) seasonal periods. The whole Mediterranean Sea presents higher *chl* values in January, February and March (period referred to as winter, in the following), with peak blooming occurring earlier (February) in a few sub-basins and systems (*e.g.* the Alboran Sea and the Algerian Current, in the western basin) or later on (March) in others (*e.g.* the Ligurian-Provençal Sea, in the western basin, but also the northeastern Levantine basin, in the area of the Rhodes Gyre). While blooming continues in some areas (*i.e.* the northwest, but also the Alboran Sea) in April, May and June (spring, in the following), signs of oligotrophic conditions appear in the eastern basin as early as March (but as late as June in the west, *i.e.* in the Tyrrhenian Sea). The oligotrophic state prevails in July, August and September (summer), everywhere in the eastern basin, except for coastal plumes, and in the interior of the western basin. Elsewhere in the western basin, the northern near-coastal area of the Ligurian-Provençal Sea seems to retain higher *chl* values, even in summer, similarly to the southern near-coastal area impacted by the incoming (permanent) Atlantic jet. These conditions appear to relax in October, November and December (fall), as early as October in the western basin, starting from the southwest, but only in December in the eastern one, when blooming seems to take up again, in preparation for the winter peak.

In the preceding analysis, the SeaWiFS-derived time series presents a seasonal cycle analogous to the one appearing in the historical CZCS data set, *i.e.* a bimodal pattern with *maxima* in the colder season, from late fall to early spring, followed by *minima* in the warmer one, from

late spring to early fall. This is substantiated by the fluctuation of the average basin value of *chl* derived from the monthly means (*i.e.* a single *chl* value computed as the total average of all pixels composing each monthly image), shown in Plate 10. As noted already for the annual means, the *chl* indicator displays also a decreasing trend, over the period of SeaWiFS coverage, estimated in this case, by linear regression, to be about 20% of the climatological average value for the entire basin.

The climatological seasonal trend (Plate 11), obtained computing an average basin value of the *chl* indicator from the climatological monthly mean images, suggests that, from a bio-geo-chemical point of view, the Mediterranean Sea as a whole presents a behaviour similar to that of a sub-tropical basin, where the light level is never a limiting factor, so that its decrease in winter does not inhibit algal growth, but the nutrient level always is (Barale, 2000). In such a scenario, higher *chl* values would occur in the cold, windy and wet (winter) season, and would be related to the biological enrichment of surface waters due to surface cooling, vertical mixing and continental runoff – as opposed to lower *chl* values occurring in the warm, calm and dry (summer) season, when the water column is strongly stratified and no nutrient supply, from coastal zones or deeper layers, is readily available.

Unlike what is seen in the historical CZCS data set, though, absolute *maxima* do not appear in January and later in (November and) December. Indeed, peak *chl* values now occur in February and March, with reduced values in January and even more so in December. Hence, the climatological seasonal cycle in the SeaWiFS-derived time series shows that, after the summer low, *chl* grows systematically in fall, only to reach its absolute *maximum* in the middle of winter and then decrease rapidly in spring, toward its summer *minimum* again. This does not affect the general validity of the sub-tropical scenario, described earlier when considering the cycle of the entire Mediterranean basin, but points to the fact that some regions, namely the western sub-basins, have a somewhat different seasonality. The difference is so pronounced, in fact, that it affects basin statistics, when integrated *chl* values are considered to summarize the behaviour of the basin as a whole.

The interannual variability of this seasonal cycle is illustrated in Plate 12, where average basin values of the *chl* indicator from corresponding monthly means are plotted against time – subdivided in winter and spring plots, in Plate 12(a), as well as summer and fall plots, in Plate 12(b). The winter plot shows that the highest average basin value of *chl* can (almost) be reached already in January, and then maintained for the following months (as in 1998, 2000 and 2002), but it can also be delayed to February (as in 2001) or even to March (as in 1999 and 2003). In spring, the *chl* values drop rapidly and systematically from winter to summer levels, in all years considered. The summer plot

shows that the lowest average basin value of *chl* is reached (almost) always in August (the only exceptions occurring in 2000 and even more so in 2001, when actually the *chl* value increased in August), but that it varies very little throughout the entire season. In fall, the *chl* values rise, again rather systematically, from summer to winter levels. Seasonal excursion of the *chl* average basin values, in a given year, can be on the order of 10-20% in winter; as high as 20-40% in spring, the largest observed; only 10% in summer; and then 20-30% in fall.

While the Mediterranean basin as a whole seems to follow such a model, significant departures occur in some areas, and in particular in the northern sub-basins. Notably, the Adriatic Sea and the Aegean Sea display a late winter and, mostly, early spring (April) enhancement in *chl* values, superimposed to the general annual trend. Local conditions describing a combination of seasonal signatures can be recognized also elsewhere, in both the western basin – where the Alboran Sea *e.g.* presents the additional feature of coastal *chl* enhancement in early spring – and in the eastern basin – where the Rhodes Gyre core, after reaching a late winter (March) *chl maximum*, maintains its characteristics throughout the year, even appearing in summer months as the only, isolated, offshore spot of high *chl* in the super-oligotrophic basin.

The Ligurian-Provençal Sea deserves a special reference, in this list of exceptions, for displaying, primarily in the Gulf of Lyon, a rather different, almost opposite, seasonal cycle. In fact, the lowest *chl* values appear in winter, and are followed by a massive bloom in March and April. This feature, the most pronounced of the entire Mediterranean Sea, continues to be identifiable even throughout summer and fall. In this area, the lower *chl* values of the winter season are originated when strong northerly Mistral winds blow from the continental landmass onto the sea, so that the resulting deep convection processes, triggered systematically by this particular wind regime, can mix surface waters down to 1500-2000 m of depth (THETIS Group, 1994). This seems to be particularly true for the Lyons Gyre, an area of deep-water formation – *i.e.* the so-called "blue hole" already seen in the historical CZCS data set – where the lack of high *chl* in winter is linked to the extreme conditions generated by the overturning of the entire water column. This seasonality would be closer to that of a sub-polar basin, rather than a sub-tropical one, with lower pigment concentration in winter, because of reduced light or actually, more important in this case, because of the deep vertical mixing and turbulence due to the prevailing wind field, which prevents algae to be stabilized in the upper well-lit layers. The ensuing spring bloom, then, would be triggered by the relaxation of these conditions, when the wind field reduces its impact, the water column – enriched in nutrient content by the prolonged period of deep convection – becomes sufficiently stable, and stratification occurs in the basin.

It must be noted, however, that the period of deep convection appeared to be longer in the CZCS climatological sequence, since the monthly mean images showed a larger "blue hole", extending also in the Ligurian Current region, from late fall to early spring. The feature, occurring earlier in December, and then most intensely in January, February and March as well, now can hardly be recognized in December, starts to become evident in January, and is obvious only in February, while extensive blooming takes place already in March. Interestingly enough, no "blue hole" was manifest in the imagery of fall of 1997 (not shown here), when the SeaWiFS time series got started. This apparent lack of deep convection in the Gulf of Lyon, was followed by the least pronounced and shortest spring bloom observed in the same area for the 6 years considered. This testifies once more the importance of wind-induced processes in the biological cycles of the northwestern Mediterranean Sea, where the enrichment of surface waters supports a large biomass of primary and secondary producers, as well as a highly developed food web including a sizeable standing population of fin whales, *Balaenoptera physalus* (see Barale *et al.*, 2002, and references therein).

3.2 Blooming Anomalies in the Monthly Means

The SeaWiFS-derived *chl* monthly anomalies shown in Plates 13-24 highlight the geographical spread and intensity of blooming patterns, which differed in each month from the corresponding climatological monthly mean. The time series shows that anomalies can occur just about anywhere in the basin, even though they are most noticeable in the areas of intense blooming, and in all periods of the year. There are at least three general types of anomalies, which seem to be of particular interest. The first is a basin-wide anomaly, when the greater part of the Mediterranean Sea appears to be above or below the climatological mean value (*e.g.* December 1998, positive; December 2002 or 2003, negative). The second kind of anomaly shows the western and the eastern basins oscillating in opposite ways (*e.g.* September 2000, western basin mainly negative, eastern mainly positive; and February 2001, opposite situation). In general, though, the most common anomalies are of a third kind, which involves only a specific sub-basin or near-coastal area. In the western basin, the Ligurian-Provençal Sea and the Alboran Gyres – Algerian Current system, where the most intense blooming occurs, are once again the sites of recurring anomalies. As an example, both positive and negative anomalies can be seen, in sequence, between February and March 1998 in these areas. In the eastern basin, the gyre system south and east of the Island of Crete, and the Rhodes Gyre in particular, displays similar characteristics (*e.g.* negative anomalies in March 1998, and positive in April 2003). Even though a general trend does not seem to be easily identifiable, it appears that short-term anomalies like those in the monthly record can provide important information about regional conditions linked to local blooming events.

Plate 9. SeaWiFS-derived chl Climatological Monthly Means

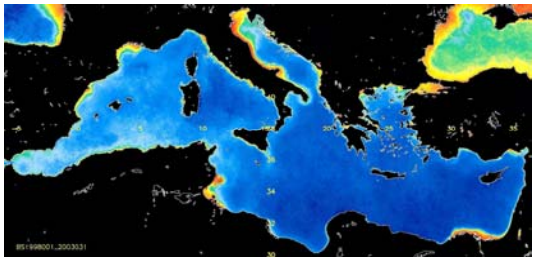

January

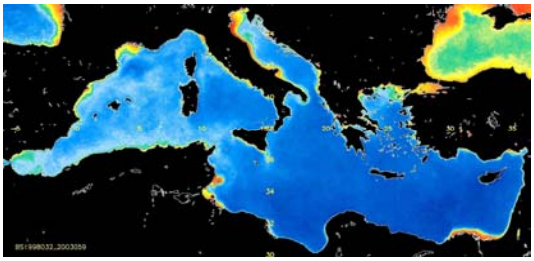

February

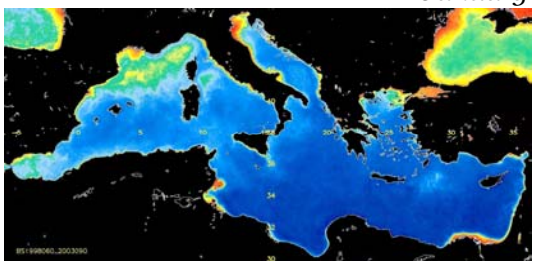

March

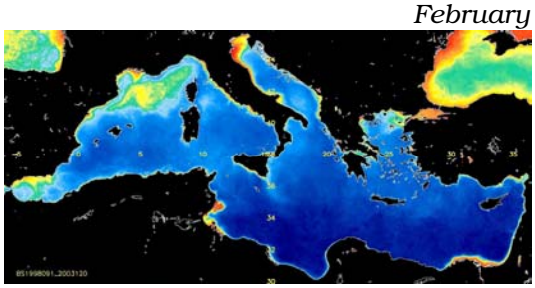

April

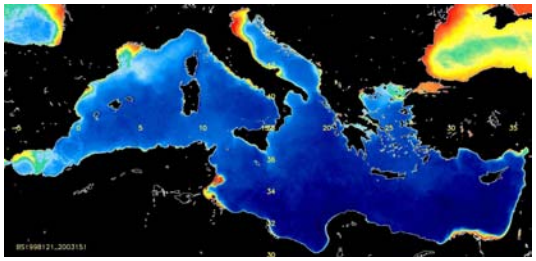

May

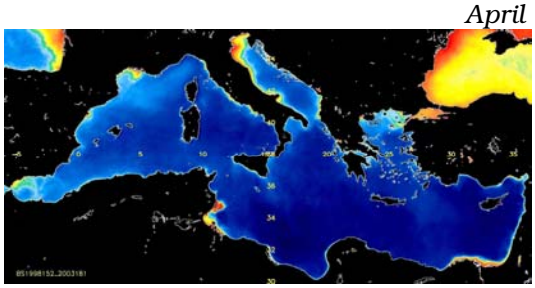

June

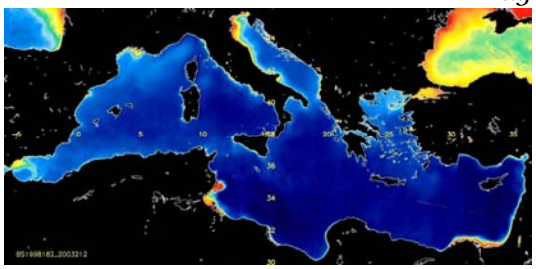

July

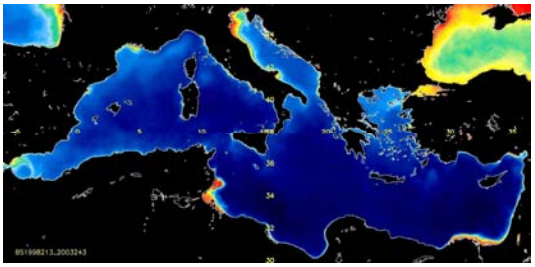

August

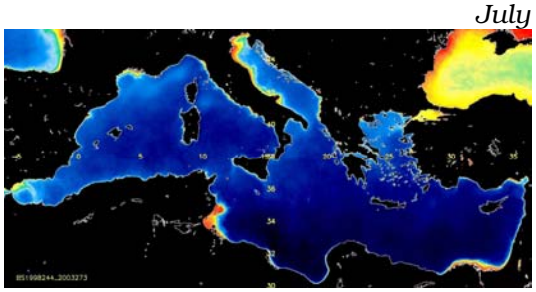

September

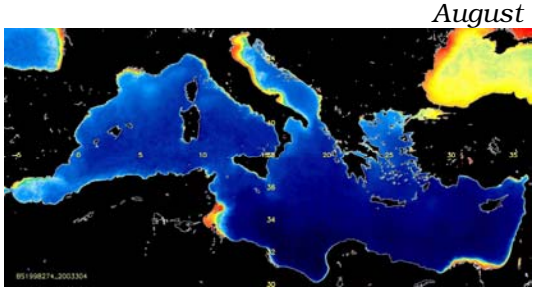

October

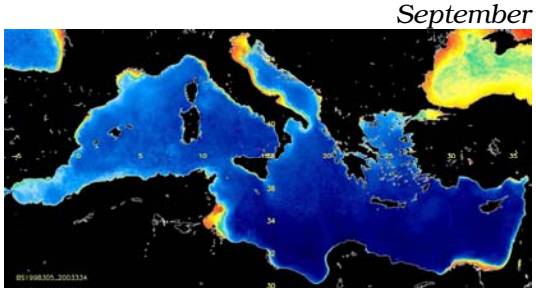

November

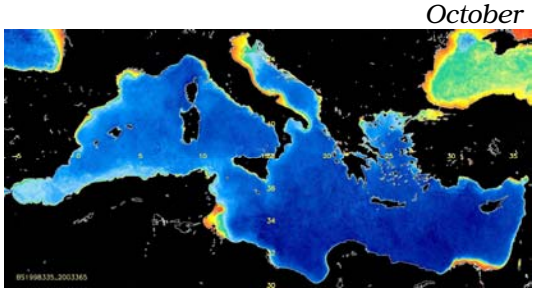

December